MAX-PLANCK-INSTITUT
FÜR PLASMAPHYSIK

Gyrokinetic simulations of MHD modes in stellarator plasmas

TSVV10 Meeting 2023-11-23

Carolin Nührenberg[1]
R. Kleiber, A. Mishchenko, A. Könies[2]
R. Hatzky[3]
M. Borchardt[4]

[1]IPP Greifswald TSVV12 [2]IPP Greifswald TSVV10 [3]IPP Garching ACH [4]IPP Greifswald

EUROfusion

This work has been carried out within the framework of the EUROfusion Consortium, funded by the European Union via the Euratom Research and Training Programme (Grant Agreement No 101052200 — EUROfusion). Views and opinions expressed are however those of the author(s) only and do not necessarily reflect those of the European Union or the European Commission. Neither the European Union nor the European Commission can be held responsible for them.

Motivation

- Stellarator optimization traditionally used[1] and still uses[2] ideal MHD proxies such as the vacuum-field magnetic well to ensure stability of the equilibria.
- Deepening the vacuum-field magnetic well comes at the expense of the plasma shape, relaxing the requirement of strong shaping could ease e.g. coil design.
- How is the time evolution of perturbations found linear-ideal-MHD unstable when studied in a wider physics picture? Linear and non-linear phases of time evolution? Saturation?
- use the gyro-kinetic model
- compare to global, linear ideal MHD stability

---

[1] J.Nührenberg et al. 1993.
[2] Drevlak et al. 2018.

Outline

- brief backgrounds
  - MHD
  - GK
- first applications and comparisons
  - equilibrium configuration
  - linear phase
  - non-linear phase
- summary and outlook

Setup of MHD calculations

+ ideal MHD model
+ study toroidal, general geometry MHD equilibria (VMEC[3], GVEC[4])
+ global MHD stability against small perturbations ξ, linear theory
  - time evolution of the *displacement vector* ξ is governed by Hermitian force operator $\mathcal{F}$ with time-independent coefficients
  - energy functional[5]: $(\boldsymbol{\xi}, \boldsymbol{\mathcal{F}}[\boldsymbol{\xi}]) = (\boldsymbol{\xi}, \rho_0 \boldsymbol{\xi})$
  - numerical treatment via Ritz-Galerkin method for tempo-spatial properties of the displacement; matrix eigenvalue problem with symmetric-definite pencil
  - realization in CAS3D[6] code: FE-spectral representations for equilibrium and perturbation quantities (similar in TERPSICHORE[7])

[3] Hirshman et al. 1986.

[4] Hindenlang et al. 2019.

[5] Bernstein et al. 1958; Hain et al. 1957.

[6] Nührenberg 2016; Schwab 1993.

[7] Fu et al. 1992.

Setup of gyrokinetic calculations

- options used in gyrokinetic PIC simulations with the EUTERPE code[8]

  + δf ansatz, $f = f_0 + \delta f$ with shifted equilibrium Maxwellian for the electrons
  + kinetic species: electrons and ions with physical mass ratio
  + gyro-average
  + non-linear, electromagnetic model
  + symplectic/Hamiltonian splitting technique, $\delta A_{||} = \delta A_{||}^s + \delta A_{||}^h$
  + full perturbed magnetic field, $\delta \mathbf{B} = \boldsymbol{\nabla} \times (\delta A_{||}\, \mathbf{b}) + \delta B_{||}\, \mathbf{b}$
  + pull-back formalism

  + B-spline representations
  + Fourier representations of potentials Φ, $\delta A_{||}$, and $\delta B_{||}$ used in field equations
  + direct solver for field equations

[8] Kleiber et al. 2023.

Equilibrium: geometrically simple stellarator

- 4-periodic $\ell = 1{,}2$ stellarator
- helical excursion of magnetic axis; plasma cross-section is turning a ellipse
- low magnetic shear and a vacuum magnetic hill drive this case unstable

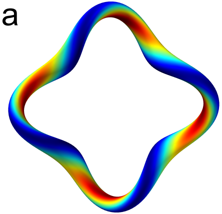

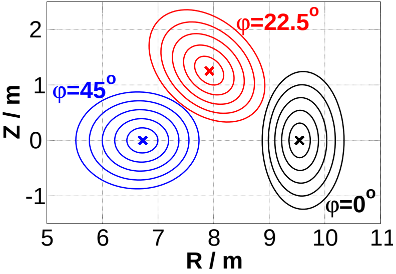

Equilibrium: geometrically simple stellarator

- 4-periodic $\ell = 1{,}2$ stellarator
- helical excursion of magnetic axis; plasma cross-section is turning a ellipse
- low magnetic shear and a vacuum magnetic hill drive this case unstable
- equilibrium: choose normalized profiles of temperatures and densities identical (on-axis values see table)

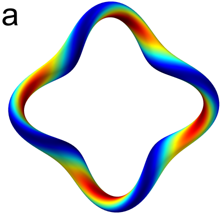

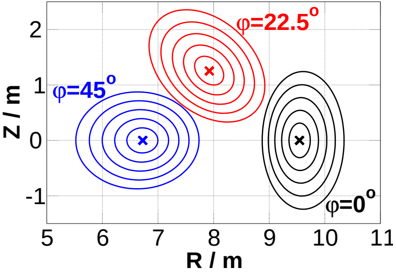

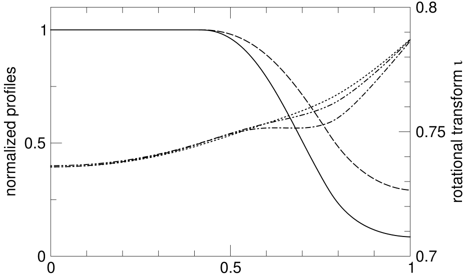

-

$T_{i,e}$ / keV	0.81	1.04	1.3
$n_{i,e}$ / $(10^{19}\ \mathrm{m}^{-3})$	2.85	3.67	4.63
$\langle\beta\rangle$	0.006	0.01	0.016

GK - MHD comparison

- study dominantly $(m, n) = (4, -3)$ perturbation
  suggested by the resonance condition being $\boxed{k_{||} \approx 0 \quad \text{or} \quad m\,\iota + n = 0}$
  breaks the 4-fold periodicity of the equilibrium
  need to treat the **full** torus as one field period in the EUTERPE code
- use identical diagonal Fourier filters in CAS3D and EUTERPE

filter adjusted to $\iota = 3/4$ with maximum 19 entries for each toroidal n; figure showing only the $n \geq 0$ part of the filter, the part for negative n is added point-symmetrically

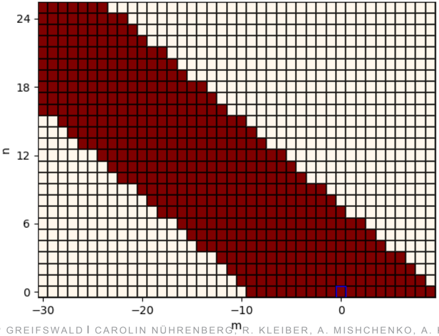

GK - MHD comparison

- study dominantly $(m, n) = (4, -3)$ perturbation
  suggested by the resonance condition being $\boxed{k_{||} \approx 0 \quad \text{or} \quad m\,\iota + n = 0}$
  breaks the 4-fold periodicity of the equilibrium
  need to treat the **full** torus as one field period in the EUTERPE code
- use identical diagonal Fourier filters in CAS3D and EUTERPE
- boundary conditions
  - fixed-boundary modes: Dirichlet boundary condition at plasma boundary
  - inner boundary
    CAS3D: Dirichlet at magnetic axis, vanishing normal displacement harmonics
    EUTERPE: check influence of inner boundary: location and type
    (i) inner boundary at magnetic axis, all Φ-harmonics with $m \neq 0$ vanish (Dirichlet), vanishing radial derivative for $m = 0$ harmonics (Neumann)
    (ii) inner boundary at $r/a = 0.2$, all Φ-harmonics vanish (Dirichlet)

New diagnostic in EUTERPE: field-line tracing

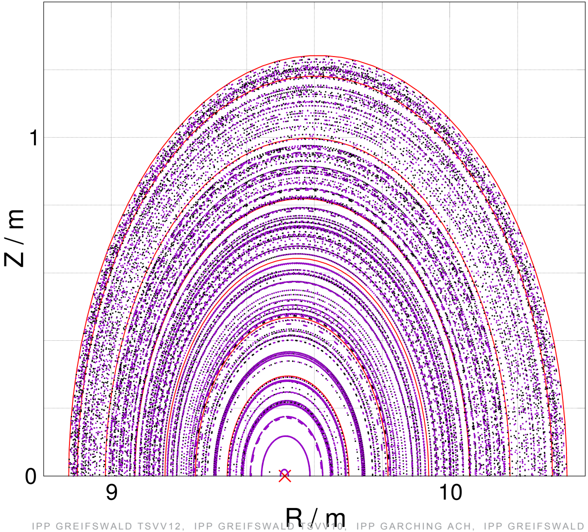

integration of electron trajectories in the given magnetic field (unperturbed or perturbed, no drifts, …)

here: **unperturbed** magnetic field of $\ell = 1, 2$ stellarator at $\langle\beta\rangle = 0.006$; half of the up-down symmetric cross-section at the beginning of a field period

GVEC equilibrium code assumes nested surfaces (solid, red lines)

EUTERPE uses background field given by GVEC (violet and black Poincaré points)

Linear phase: growth rates

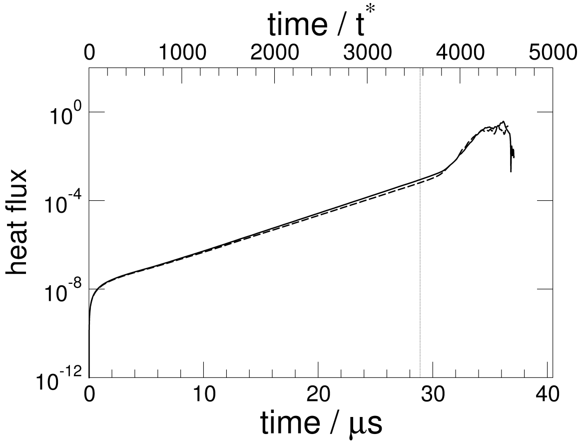

EUTERPE for $\ell = 1{,}2$ stellarator at $\langle \beta \rangle = 0.016$:
inner boundary $\rho = 0 \;\; (0.2)$: dashed (solid).
Markers: 300 (600) mio. ions (electrons)

	growth rate $/(\mu\text{s})^{-1}$	frequency /kHz
gyrokinetics	0.1909	-19.51
ideal MHD	0.2013	22^{*}

* electron diamagnetic drift frequency

$$\omega_{n,\mathrm{e}} = \mathbf{k} \cdot \mathbf{v}_{\mathrm{de}} = \frac{T_\mathrm{e}\, k_\theta}{e\, B\, L_n}$$

since here the pressure and temperature profiles are chosen to be the same:

$$\omega_{n,\mathrm{e}} = \omega_{T,\mathrm{e}} = \frac{1}{2}\, \omega_{p,\mathrm{e}}$$

the sign remains to be discussed

Linear phase: electrostatic potential

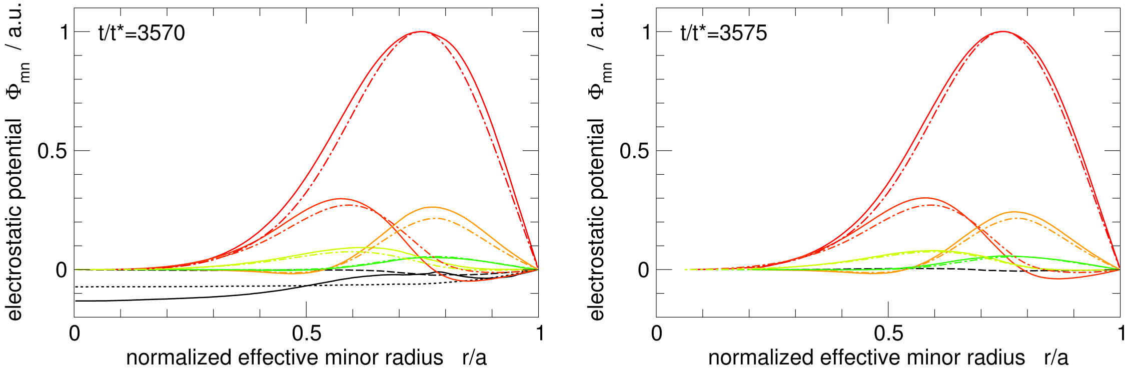

Strongest Fourier harmonics of the electrostatic potential, Re(Φ), for $\ell = 1{,}2$ stellarator at $\langle\beta\rangle = 0.016$
left (right) frame: inner boundary condition at $\rho = 0 \ \ (0.2)$; GK (i-MHD): solid (dot-dashed);
coloured: $(m, n) = (4, -3)$ and side-bands; black: $m = 0$ harmonics

Importance of terms in non-linear phase

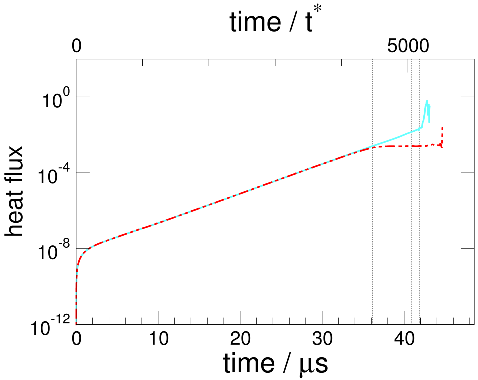

EUTERPE for $\ell = 1{,}2$ stellarator at $\langle\beta\rangle = 0.006$:
with (without) magnetic flutter: red (cyan).
Markers: 150 (300) mio. ions (electrons)

- obviously, a non-negligible $\delta\mathbf{B}$ is critical for the motion of the markers
- inclusion of magnetic flutter is needed for reaching saturation (red curve)
- in this i-MHD-unstable case, $\delta\mathbf{B}_{\|}$-terms can be omitted from the gyrokinetic simulation without changing the results
  - in i-MHD, the magnetic-field compression vanishes to very good approximation for unstable modes;
    for small equilibrium pressure gradient:
    $B\,[-\boldsymbol{\nabla}\cdot\boldsymbol{\xi}_\perp - 2\,\boldsymbol{\xi}_\perp\cdot\boldsymbol{\kappa}_\perp] \approx \delta\mathbf{B}_{\|}$

Saturation phase

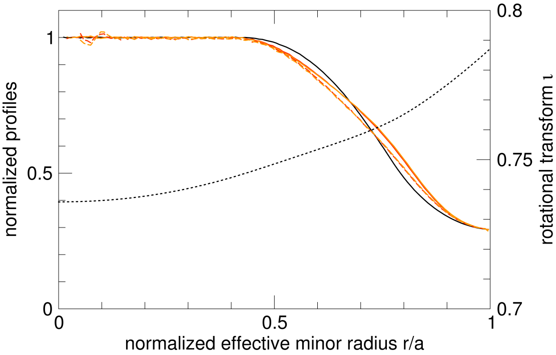

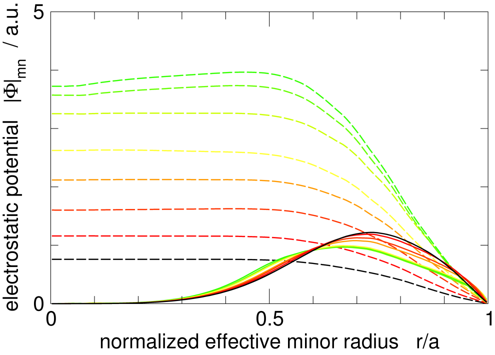

Evolution of ion temperature (solid) and density (dashed) profiles; $t/t^* = 0,\ 5050,\ 5170$: black, red, orange. EUTERPE for $\ell = 1{,}2$ stellarator at $\langle\beta\rangle = 0.006$: Markers: 150 (300) mio. ions (electrons)

Evolution of the two strongest $|\Phi|$-harmonics, $|\Phi|_{0,0}$ and $|\Phi|_{4,-3}$ (dashed, solid); $t/t^* = 4500, \ldots, 5170$: black to light green

Summary and outlook

- linear gyrokinetic study of stellarator configuration found unstable according to linearized ideal MHD
- GK: non-linear, electromagnetic, kinetic electrons with physical electron ion mass ratio, for periodicity-breaking perturbation in stellarator equilibrium
- first results in geometrically simple spatial-axis stellarator
- very good agreement of GK-linear-phase and linear-ideal-MHD growth rates and Fourier coefficients of electrostatic potential for global, spatially extended mode
- parallel field perturbation plays no role in simulation of i-MHD-unstable equilibrium
- magnetic flutter critical for reaching saturation in gyrokinetic simulation of i-MHD-unstable equilibrium
- in saturation phase: saturation of profile flattening and unstable component amplitude; zonal-flow component grows
- started simulation of shaped Helias configuration with W7-X-CERC-type profiles

BACKUP SLIDES

GK: equations of motion in mixed formulation

$$u_\parallel \equiv v_\parallel + \frac{q}{m}\langle \delta A_\parallel^h \rangle \qquad B_\parallel^* = B + \left[\frac{m}{q}u_\parallel + \langle \delta A_\parallel^s \rangle\right] \mathbf{b}\cdot(\boldsymbol{\nabla}\times\mathbf{b}) \qquad \dot{\mu} = 0 \;\Rightarrow\; \dot{v_\perp} = \frac{v_\perp}{2B}\dot{\mathbf{R}}\cdot\boldsymbol{\nabla}B$$

$$\dot{\mathbf{R}} = u_\parallel \mathbf{b} + \frac{m}{q}\left[\frac{\mu}{B_\parallel^*}\mathbf{b}\times\boldsymbol{\nabla}B + \frac{u_\parallel^2}{B_\parallel^*}\mathbf{b}\times\boldsymbol{\kappa}\right] - \frac{q}{m}\langle \delta A_\parallel^h \rangle \mathbf{b} + \frac{1}{B_\parallel^*}\mathbf{b}\times\boldsymbol{\nabla}\left\langle \Phi - u_\parallel(\delta A_\parallel^h + \delta A_\parallel^s)\right\rangle + \frac{m}{q}\frac{\mu}{B_\parallel^*}\mathbf{b}\times\boldsymbol{\nabla}\delta B_\parallel$$
$$+ \frac{u_\parallel}{B_\parallel^*}\left(\langle \delta A_\parallel^s \rangle - \langle \delta A_\parallel^h \rangle\right)\mathbf{b}\times\boldsymbol{\kappa} + \frac{q}{m}\frac{1}{B_\parallel^*}\langle \delta A_\parallel^h \rangle\left[\mathbf{b}\times\boldsymbol{\nabla}\left(\langle \delta A_\parallel^s \rangle + \langle \delta A_\parallel^h \rangle\right) - \langle \delta A_\parallel^s \rangle\,\mathbf{b}\times\boldsymbol{\kappa}\right] + \frac{1}{B_\parallel^*}\mathbf{b}\times\boldsymbol{\nabla}\Phi_0$$

$$\dot{u_\parallel} = -\mu\,\boldsymbol{\nabla}B\cdot\left[\mathbf{b} + \frac{m}{q}\frac{u_\parallel}{B\,B_\parallel^*}(\boldsymbol{\nabla}\times\mathbf{B})_\perp\right] + \frac{q}{m}\frac{u_\parallel}{B_\parallel^*}\left[\mathbf{b}\times\boldsymbol{\nabla}\langle \delta A_\parallel^h \rangle\cdot\boldsymbol{\nabla}\langle \delta A_\parallel^s \rangle + \left(\langle \delta A_\parallel^s \rangle - \langle \delta A_\parallel^h \rangle\right)\mathbf{b}\times\boldsymbol{\kappa}\cdot\boldsymbol{\nabla}\langle \delta A_\parallel^h \rangle\right]$$
$$- \frac{\mu}{B_\parallel^*}\left[\mathbf{b}\times\boldsymbol{\nabla}B\cdot\boldsymbol{\nabla}\langle \delta A_\parallel^s \rangle + \frac{\langle \delta A_\parallel^s \rangle}{B}\boldsymbol{\nabla}B\cdot(\boldsymbol{\nabla}\times\mathbf{B})_\perp\right] + \frac{q}{m}u_\parallel\,\mathbf{b}\cdot\boldsymbol{\nabla}\langle \delta A_\parallel^h \rangle - \frac{u_\parallel}{B_\parallel^*}\mathbf{b}\times\boldsymbol{\kappa}\cdot\boldsymbol{\nabla}\langle \Phi - u_\parallel\delta A_\parallel^h \rangle$$
$$- \frac{q}{m}\frac{1}{B_\parallel^*}\left[\mathbf{b}\times\boldsymbol{\nabla}\langle\Phi\rangle\cdot\boldsymbol{\nabla}\langle \delta A_\parallel^s \rangle + \langle \delta A_\parallel^s \rangle\,\mathbf{b}\times\boldsymbol{\kappa}\cdot\boldsymbol{\nabla}\langle\Phi\rangle\right] - \frac{q^2}{m^2}\langle \delta A_\parallel^h \rangle\mathbf{b}\cdot\boldsymbol{\nabla}\langle \delta A_\parallel^h \rangle$$
$$- \mu\left[\mathbf{b} + \frac{m}{q}\frac{u_\parallel}{B_\parallel^*}\mathbf{b}\times\boldsymbol{\kappa}\right]\cdot\boldsymbol{\nabla}\delta B_\parallel - \frac{u_\parallel}{B_\parallel^*}\mathbf{b}\times\boldsymbol{\kappa}\cdot\boldsymbol{\nabla}\Phi_0 + \frac{q}{m}\frac{1}{B_\parallel^*}\left[\mathbf{b}\times\boldsymbol{\nabla}\langle \delta A_\parallel^s \rangle - \langle \delta A_\parallel^s \rangle\mathbf{b}\times\boldsymbol{\kappa}\right]\cdot\boldsymbol{\nabla}\Phi_0$$

GK: weight and field equations

weight equation

$$\dot{w}_s = -\Omega_p S_s, \qquad S_s = \dot{\mathbf{R}}\cdot\boldsymbol{\nabla} f_{0,s} + \dot{u}_\parallel \frac{\partial f_{0,s}}{\partial v_\parallel} + \dot{v}_\perp \frac{\partial f_{0,s}}{\partial v_\perp} \quad \text{with} \quad \dot{v}_\perp = \frac{v_\perp}{2B}\dot{\mathbf{R}}\cdot\boldsymbol{\nabla} B$$

$$f_{0,s} = \frac{n_{0s}(\mathbf{x})}{(2\pi)^{\frac{3}{2}}\, v_{\mathrm{th},s}^3} \exp\left(-\frac{v_\parallel^2 + v_\perp^2}{2\, v_{\mathrm{th},s}^2}\right) \quad \text{where} \quad v_{\mathrm{th},s}^2(\mathbf{x}) = \frac{T_s(\mathbf{x})}{m_s}$$

Quasi neutrality

$$\sum_s q_s\, n_s = 0, \qquad n_s = \langle n_s \rangle + \frac{m_s}{q_s}\boldsymbol{\nabla}\cdot\left(\frac{n_{0s}(\mathbf{x})}{B^2}\boldsymbol{\nabla}_\perp \Phi\right)$$

Ampère's law

$$-\frac{1}{\beta}\boldsymbol{\nabla}\cdot\boldsymbol{\nabla}_\perp \delta A_\parallel^h + \sum_s n_{0s}(\mathbf{x})\frac{q_s^2}{m_s\,\delta A_\parallel^h} = \sum_s \langle j_{\parallel,s}\rangle + \frac{1}{\beta}\boldsymbol{\nabla}\cdot\boldsymbol{\nabla}_\perp \delta A_\parallel^s$$

Ohm's law

$$\frac{\partial \delta A_\parallel^s}{\partial t} + \mathbf{b}\cdot\boldsymbol{\nabla}\Phi = 0$$

pressure balance

$$-\frac{B}{\beta}\,\delta B_\parallel = \sum_s p_{\perp,s} \qquad \text{here} \quad m_s = \frac{m_{\mathrm{p,e}}}{m_{\mathrm{p}}} \quad \text{and} \quad q_s = \frac{q_{\mathrm{p,e}}}{|e|}$$

Equilibrium: 4-period Helias

- 4-periodic $\ell = 1{,}2$ Helias
- helical excursion of magnetic axis; shaped plasma-boundary with indentation

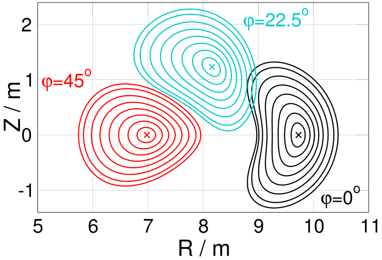

Equilibrium: 4-period Helias

- 4-periodic $\ell = 1{,}2$ Helias
- helical excursion of magnetic axis; shaped plasma-boundary with indentation
- profiles similar to CERC case in W7-X; on-axis values in table
-

T_e / keV	1.612
T_i / keV	1.247
$n_{i,e}$ / $(10^{19}$ m$^{-3})$	4.773
$\langle\beta\rangle$	0.010

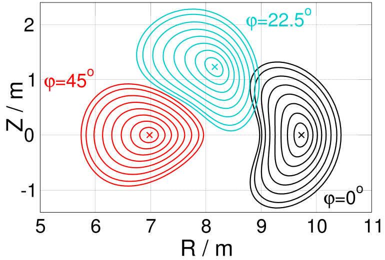

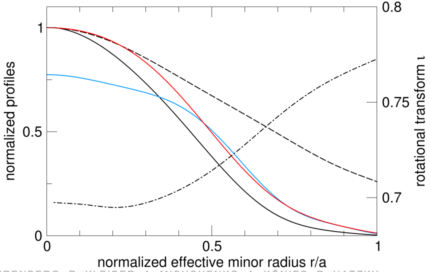

Some results for Helias case

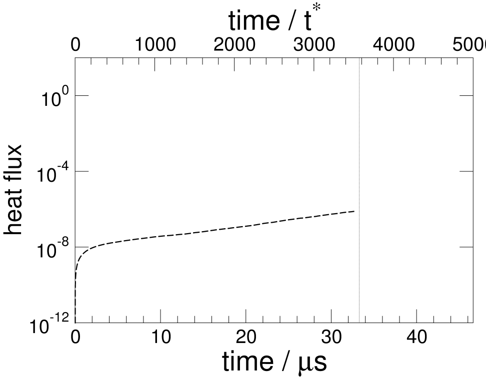

EUTERPE for 4-period Helias at $\langle\beta\rangle = 0.01$;
markers: 300 (600) mio. ions (electrons)

growth rate	gyrokinetics	ideal MHD
$/(\mu s)^{-1}$	0.074	0.095

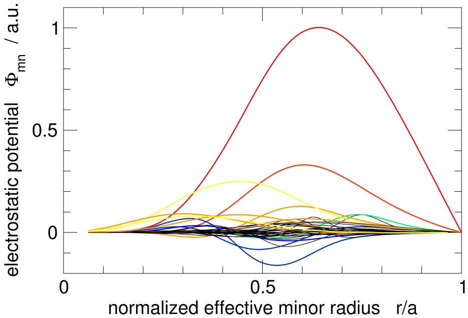

i-MHD from CAS3D: Strongest Fourier harmonics of the electrostatic potential, Re(Φ)
coloured: $(m, n) = (4, -3)$ and side-bands;
black: higher-m harmonics